

# Silicon detector array for radioactive beam experiments at HIRFL-RIBLL

Fang-Fang Duan<sup>1,2</sup> · Yan-Yun Yang<sup>2</sup> · Bi-Tao Hu<sup>1</sup> · Jian-Song Wang<sup>2</sup> · Zhi-Hao Gao<sup>2</sup> · Xing-Quan Liu<sup>2</sup> · Dipikap Patel<sup>2</sup> · Peng Ma<sup>2</sup> · Jun-Bing Ma<sup>2</sup> · Shu-Ya Jin<sup>2</sup> · Zhen Bai<sup>2</sup> · Qiang Hu<sup>2</sup> · Guo Yang<sup>2</sup> · Xin-Xin Sun<sup>1</sup> · Nan-Ru Ma<sup>3</sup> · Li-Jie Sun<sup>4</sup> · Hui-Ming Jia<sup>3</sup> · Xin-Xing Xu<sup>3,5</sup> · Cheng-Jian Lin<sup>3</sup>

Received: 25 July 2018 / Revised: 22 August 2018 / Accepted: 27 August 2018 / Published online: 4 October 2018  
© Shanghai Institute of Applied Physics, Chinese Academy of Sciences, Chinese Nuclear Society, Science Press China and Springer Nature Singapore Pte Ltd. 2018

**Abstract** A new and innovative detector system based on a silicon strip detector dedicated to the study of the reaction induced by lighter radioactive beams is described herein. The detector system consists of five sets of three types of telescopes, which are successfully used to measure the angular distributions of both elastic scattering and breakup simultaneously, on the Radioactive Ion Beam Line in Lanzhou at Heavy Ion Research Facility in Lanzhou. This silicon detector array is used to measure the elastic scattering angular distributions of  $^{11}\text{Be}$  on a  $^{208}\text{Pb}$  target at  $E_{\text{lab}} = 140$  and 209 MeV. A comparison of the Monte Carlo simulations with the experimental results shows a reasonable consistency.

**Keywords** Direct nuclear reactions · Silicon detector array · Radioactive ion beams · Monte Carlo simulation

## 1 Introduction

The reactions of weakly bound nuclei have been investigated over the past few decades. The nuclei far from the  $\beta$ -stability line show peculiar features in contrast to stable nuclei [1–4]. The reactions induced by exotic nuclei offer the opportunity to explore the unusual features of nuclear structures such as the properties of exotic nuclei, which are usually weakly bound, and the proton-to-neutron ratio, which is different from that of the stable ones. To construct nuclear models to describe the detailed properties of nuclei, the direct nuclear reactions, such as elastic scattering, inelastic scattering, breakup, and transfer reaction, have been carried out for further studying the exotic nuclear structure [5, 6]. A direct nuclear reaction is a simple process for the deep understanding of the interaction potentials and density distributions of nuclei. Thus, it becomes an ideal tool to explore the properties of nuclei by comparing the similarities and differences in reactions caused by weakly bound nuclei and stable ones.

With the development of radioactive beam facilities [7, 8], several exciting results related to the understanding of fundamental nuclear physics were obtained. However, typical beam intensities are low and the production is often undertaken in a very small quantity. Therefore, a new generation of detectors should be designed with a large solid angle and angular coverage, and they should be able to identify particles effectively with high energy resolution, high spatial resolution, and high geometric efficiency. Silicon strip detectors, which have the characteristics of

---

This work was supported by the National Natural Science Foundation of China (Nos. U1432247, 11575256, and U1632138), the CAS program of Light of West China Program under Grant (No. Y601030XB0), and the National key R&D Program of China (No. 2018YFA0404403).

---

✉ Yan-Yun Yang  
yangyanyun@impcas.ac.cn

- <sup>1</sup> School of Nuclear Science and Technology, Lanzhou University, Lanzhou 730000, China
- <sup>2</sup> Institute of Modern Physics, Chinese Academy of Sciences, Lanzhou 730000, China
- <sup>3</sup> Department of Nuclear Physics, China Institute of Atomic Energy, Beijing 102413, China
- <sup>4</sup> School of Physics and Astronomy, Shanghai Jiao Tong University, Shanghai 200240, China
- <sup>5</sup> Department of Physics, The University of Hong Kong, Hong Kong, China

high detection efficiency and high energy resolution, have become universal devices for telescope arrays used at radioactive ion beam (RIB) facilities. Moreover, a double-sided silicon strip detector (DSSD), with highly segmented strips on the front (junction) side perpendicular to those on the back (ohmic) side, is very useful for studying the angular distributions of direct nuclear reactions. Many silicon detector arrays have been developed in international laboratories—for instance, MUST2 [9, 10], TIARA [11], and GLORIA [12]. Moreover, our domestic laboratories have developed some detector setups [13–15] to study nuclear physics and astrophysics induced by weakly bound nuclei. DSSDs, such as Louvain–Edinburgh detector array [16] and compact disk DSSD array [17], have already been successfully applied in elastic scattering experiments. These experiments of weakly bound nuclei on medium- or heavy-mass targets have been performed, and many interesting phenomena have been observed by studying their angular distributions of elastic scattering at energies near the Coulomb barrier. However, the experimental data for weakly bound nuclei above the Coulomb barrier are still scarce.

A new detector based on DSSD is designed for the study of the reaction products in a direct nuclear reaction experiment at energies above the Coulomb barrier on the Radioactive Ion Beam Line in Lanzhou (RIBLL) [18, 19] at the Heavy Ion Research Facility in Lanzhou (HIRFL) [20, 21]. Notably, RIBLL is a high-performance projectile fragmentation-type radioactive ion beam (RIB) facility with large acceptances and solid angle. However, the disadvantage of RIBLL is that it has a broad distribution in coordinate spaces. In this work, a new detector system with high resolution and a large solid angle was successfully developed for performing a nuclear reaction experiment using RIBs. The geometric efficiency of the new detector array with five large-area DSSD telescopes increased up to 70%. A detailed description of each telescope is presented in Sect. 2. Section 3 describes the electronics and data acquisition system. This silicon array was first applied in an experiment of elastic scattering of  $^{11}\text{Be}$  on a  $^{208}\text{Pb}$  target at energies of 140 and 209 MeV on RIBLL at the HIRFL. The results are compared with the Monte Carlo simulations, as discussed in Sects. 4 and 5. Some concluding remarks are presented in Sect. 6.

## 2 Design of the detector array

To measure the angular distributions of elastic scattering and breakup at energies three times above the Coulomb barrier, the requirements for the design were imposed as follows:

- *Energy resolution* There are many factors that can affect the energy resolution, such as target thickness and beam spot size. Hence, the energy resolutions of different DSSDs must be implemented in a proper energy calibration procedure in the analysis program.
- *Particle identification* One of the most essential tasks in nuclear physics experiments is particle identification, especially for nuclear reactions. Light-charged particles are identified by means of a thin energy loss ( $\Delta E$ ) stage and a much thicker residual energy ( $E$ ) detector in which the particles are stopped. This method involves building a particle identification telescope using the  $\Delta E - E$  method. The present detection system consists of five  $\Delta E - E$  telescopes, consisting of one DSSD with the thickness of 150  $\mu\text{m}$  as the  $\Delta E$  detector, and a square silicon detector (SSD) with the thickness of 1500  $\mu\text{m}$  as the  $E$  detector. The DSSDs and SSDs used in the new detector system are ion-implanted, passivated equipment produced by Micron Semiconductor Ltd. in the UK. The energy resolutions of the DSSDs and SSDs were measured using 5.486 MeV  $\alpha$  particles from a  $^{241}\text{Am}$  source and they satisfy the experimental requirements. A full width at half maximum (FWHM) overall resolution of 1.0% was achieved. We measured the full depletion voltage for each detector as it is required to achieve complete charge collection.
- *Angular range* The present detector system is expected to be applied to measure the elastic scattering and breakup cross sections at energies three times above the Coulomb barrier. The characteristics of the angular distribution of elastic scattering products show oscillatory nature within a certain angle range. This angular range covers the smallest scattering angle where the ratio of the differential elastic scattering cross sections is equal to 1/4 the pure Rutherford scattering. Therefore, particles with angles smaller than  $30^\circ$  should be detected.
- *Angular resolution* To obtain the angular distribution of the differential cross section of the experiment for breakup and elastic scattering at energies three times above the Coulomb barrier, a successful implementation of the detector system for charged particles is required. The system should be capable of identifying the charged particles over a wide energy range and measuring the energy with the resolution of 100 keV and angles better than  $1^\circ$ . In the detector array, the strip pitches of the DSSDs are 3, 2, and 0.76 mm, and the distance is 300 mm from the target to the center of the detector system. It is available at a reasonable cost, and therefore, this option is a convenient choice for our design.

- Detector geometry** The detector system was designed with a very compact geometry so that it can be fixed on stainless-steel plates to reduce systematic uncertainties. Angular overlapping regions between adjacent telescopes existed in order to provide a continuous angular distribution. The configuration of the detector array is shown in Fig. 1. The detector array consists of five  $\Delta E - E$  particle telescopes, denoted as Tel1, Tel2, Tel3, Tel4, and Tel5. Tel1 is placed on top, Tel2 and Tel3 are placed at the left and right, respectively, and Tel4 and Tel5 are placed below. Five detectors with a large area are used in order to cover large solid angles and obtain more quantities, which would be an advantage for data analysis. The detector system not only improves the geometrical efficiency but also allows modularization. The pre-amplifiers between two aluminum blocks are capable of operating in vacuum adjacent to the detectors, so as to minimize the influence of cable capacitance. As the resolution of the detectors has a strong temperature dependence, it is necessary to cool the array during the experiment.

The first stage DSSD of Tel1 consists of 128 horizontal strips and 128 vertical strips, backed by a  $100.5 \times 100.5 \text{ mm}^2$  SSD. Each strip has an active area with a length of 97.22 mm and width of 0.7 mm. The distance from the center of Tel1 to the center of the lead target is 267.82 mm. The angular range covered by Tel1 is  $7^\circ$  to  $26^\circ$ , whereas the angular resolution of DSSD of Tel1 is  $0.15^\circ$ .

The DSSDs in Tel2 and Tel3 have 32 elements ( $X$  position) in the junction side and 32 elements ( $Y$  position) in the ohmic side, the strips are 65.18 mm in length and 2 mm in width, and the area of the total active region is

$65.18 \times 65.18 \text{ mm}^2$ . Further, each DSSD is backed by an SSD with the same active area. The distance from the center of Tel2 or Tel3 to the center of the target is 272.38 mm. Notably, these two telescopes can obtain a continuous angular range between  $13^\circ$  and  $26^\circ$ , and their angular resolutions are  $0.39^\circ$ .

The DSSDs in Tel4 and Tel5 have 16 elements each in the junction and ohmic sides, whose strips have a length of 51.2 mm and a pitch size of 3 mm. Each detector has a surface area of  $51.2 \times 51.2 \text{ mm}^2$ . They are also followed by SSDs with the same area. The distance from the center of Tel4 or Tel5 to the center of the target is 287.76 mm, and their angular coverage ranges are from  $11.6^\circ$  to  $22.5^\circ$ , and their angular resolutions are  $0.6^\circ$ .

The layout of the experimental setup of elastic scattering and breakup measurements is shown in Fig. 2. Five sets of  $\Delta E - E$  telescopes are used to measure the reaction products. For this detector system, the geometric efficiency reaches up to 70%. To accurately measure the position and direction of the beam, two DSSDs of 87 and 68  $\mu\text{m}$  with 16 horizontal and 16 vertical strips were installed in front of the target. Here, by using two DSSDs instead of parallel-plate avalanche counters, the detection efficiency in front of the target reaches 100%.

### 3 Electronics and data acquisition system

A crucial aspect of this project was to obtain good energy resolution of the detectors in any associated electronics. As mentioned before, the entire detector system has 453 signals to be amplified, shaped, and digitalized. The numerous channels in the detector system were

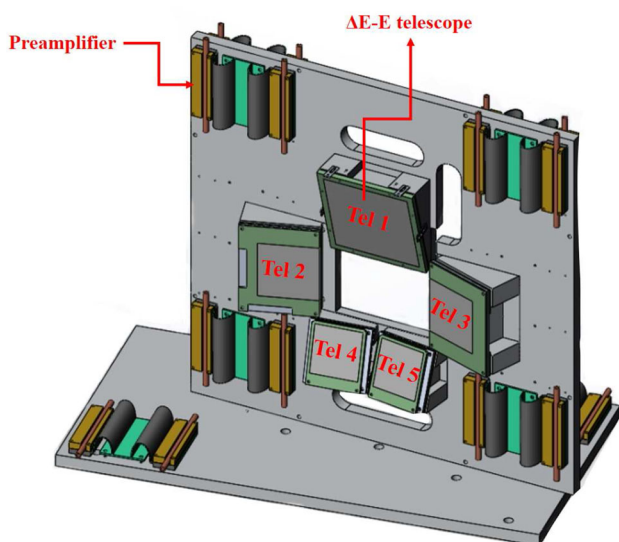


**Fig. 1** (Color online) Schematic view of the new detector array

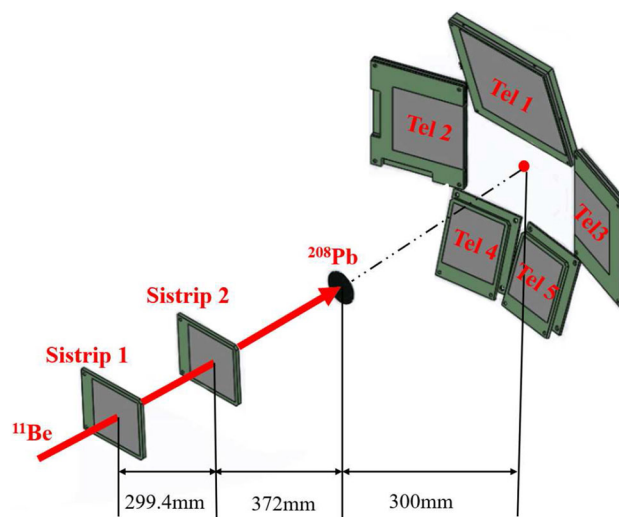


**Fig. 2** (Color online) Schematic view of the detector setup

controlled using a VME and NIM data acquisition system for telescopes.

The five SSDs have only five signals, which were amplified by three Mesytec MPR-16 amplifiers placed in the target chamber. Their energy dynamic ranges from 300 to 1500 MeV. One of the three amplifiers is used for the SSD of Tel1, one is used for the SSDs of Tel2 and Tel3, and the final one is used for the SSDs of Tel4 and Tel5. These pre-amplifiers were placed in the target chamber and cooled by the circulation of cold alcohol. Subsequently, the signals of the SSDs were sent to MSCF-16 and divided into two kinds, one of which was input into an analog-to-digital converter (ADC), and the other was used to provide a trigger for the logic chain.

The DSSD detectors produce 448 signals in total, and are equipped with pre-amplifiers developed and manufactured by China Institute of Atomic Energy. The detector system must use 28 pre-amplifiers, and each of them consists of 16 channels. The pre-amplifiers have the advantages of low noise, good linearity, high integrity, and small volume. Owing to the number of channels involved and the space constraints, our tests demonstrated that pre-amplifiers are suitable for our detection system. From Fig. 1, we can observe that all pre-amplifiers were mounted between two aluminum blocks, connected with each other through an aluminum tube, and fixed on stainless-steel plates as close as possible to the detectors in order to improve signal-to-noise ratio. To achieve the best possible resolution, it is necessary for the system to be cooled by the circulation of cold alcohol at  $-10^{\circ}\text{C}$ . This approach cools not only pre-amplifiers but also the entire system. The bias of the detectors is supplied by a Mesytec MHV-4 power supply. Energy signals from the pre-amplifiers are sent to MSCF-16 amplifiers, which can shape and amplify the energy signals, and they are subsequently digitized by the ADC module. The ADCs are triggered by the triggers from MSCF and record signals event by event.

The signal gain of the data acquisition was adjusted by using an alpha source to guarantee that all the strip energies were maintained at approximately 500 channels before the experiment started.

#### 4 Monte Carlo simulations

Monte Carlo simulations were performed by means of GEANT4 [22–24]. The entire geometry of the new detector system including the  $^{208}\text{Pb}$  target and five two-stage telescopes was implemented. Every DSSD has the same thickness of  $150\ \mu\text{m}$  and every Si detector has the thickness of  $1500\ \mu\text{m}$  in this simulation. For the first analysis of the detector response, we used a simple event generator to

produce heavy ions at the target position. For the energy distribution, we have chosen a Gaussian shape with a large width to cover a wide range of energies. The energies of proton, deuteron, and triton vary from 4 to 16, 5.5 to 22, and 6 to 25 MeV, respectively. The energies of  $^{3,4,6}\text{He}$  vary from 14 to 57, 16 to 64, and 19 to 77 MeV, respectively. The energies of  $^{7,8,9}\text{Li}$  vary from 33 to 129, 35 to 135, and 37 to 142 MeV, respectively. The energies of  $^{7,8,9}\text{Be}$  vary from 50 to 160, 52 to 160, and 55 to 160 MeV, respectively. The energies of  $^{11,12,13}\text{B}$  vary from 72 to 180, 74 to 180, and 76 to 180 MeV, respectively. The energies of  $^{11,12,13}\text{C}$  vary from 86 to 200, 89 to 200, and 92 to 200 MeV, respectively. We chose the means of the maximums and minimums as the center of the Gaussian distribution and  $3\sigma$  is equal to 40% of the mean energy. The ion is produced event-by-event evenly within a circle with the diameter of 30 mm at the target position. In the simulations, the intrinsic energy resolution of the Si detector is used.

A bidimensional spectrum  $\Delta E$  vs.  $E_{\text{total}}$  for the DSSD-Si telescope is shown in Fig. 3. The banana-like regions correspond to various test isotopes from H to  $^{13}\text{C}$ . These bands are evident.

The simulated geometrical efficiencies of the DSSD-Si telescopes are shown in Fig. 4. The geometrical efficiency is defined as the ratio of the detected particles to the emitted particles, as a function of the observed angles. The simulations confirm that the array can provide an angular coverage from  $6^{\circ}$  to  $28^{\circ}$ . For the entire array, the geometrical efficiency reaches the maximum at  $\theta = 16^{\circ}$ .

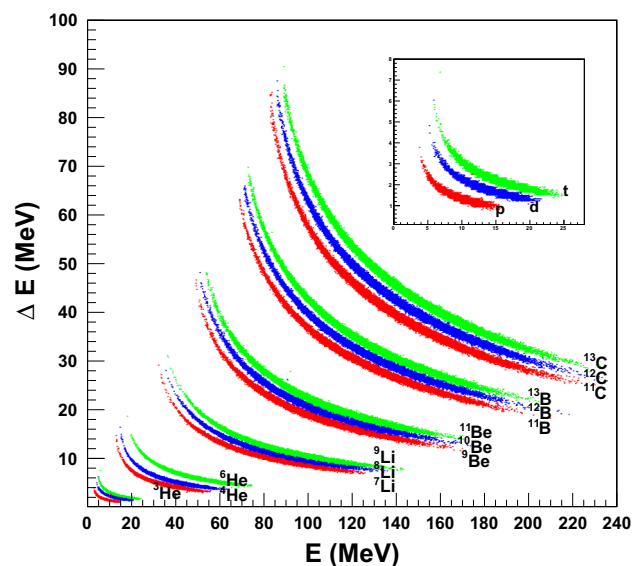


**Fig. 3** (Color online) Monte Carlo simulation of detector response for lighter ions. The expected mass spectrum of DSSD-Si telescopes is shown. Each band is marked with the corresponding nuclide

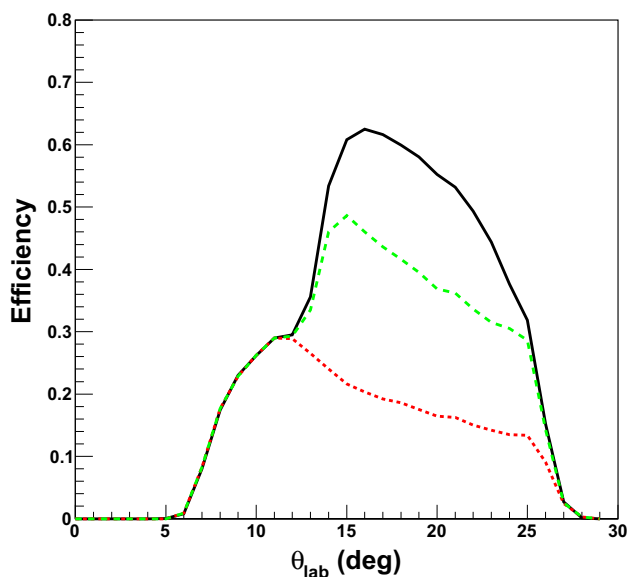
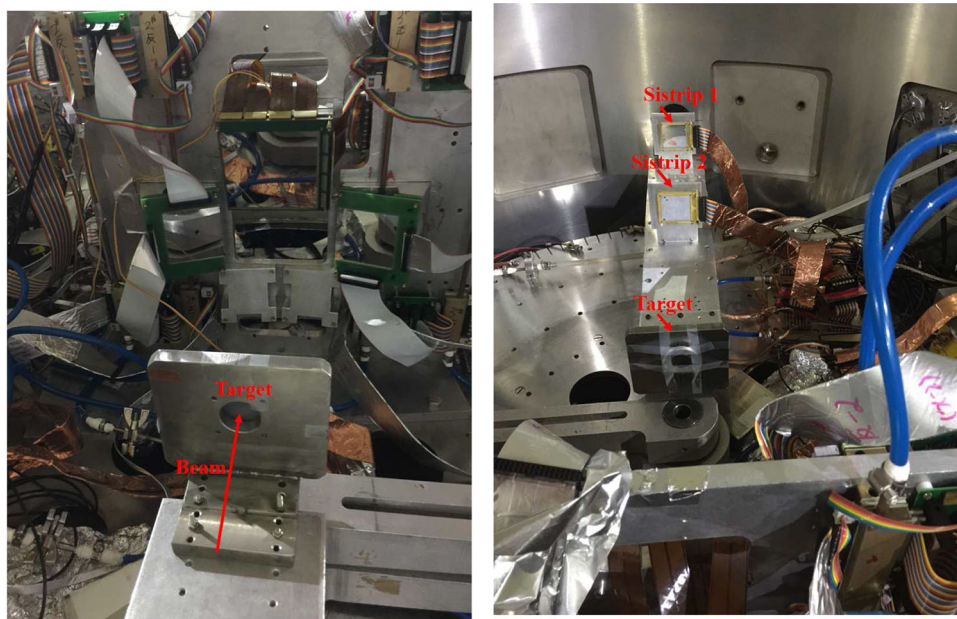


**Fig. 4** (Color online) Angular distribution of geometrical efficiency. Red dash line: Angular distribution of geometrical efficiency of Tel1. Green dash line: Angular distribution of geometrical efficiency of Tel1, Tel2, and Tel3. Black solid line: Angular distribution of geometrical efficiency of the entire array

## 5 First experimental results from the silicon detector array using the radioactive ion beams

The silicon detector array was commissioned in October 2017 on the RIBLL at the HIRFL. The aim of the experiment was to measure the angular distributions of elastic scattering and breakup when the radioactive beam of  $^{11}\text{Be}$  bombarded on a  $^{208}\text{Pb}$  target at energies of 140 and 209 MeV. The experimental setup in the reaction chamber is

**Fig. 5** (Color online) Detector system mounted in reaction chamber

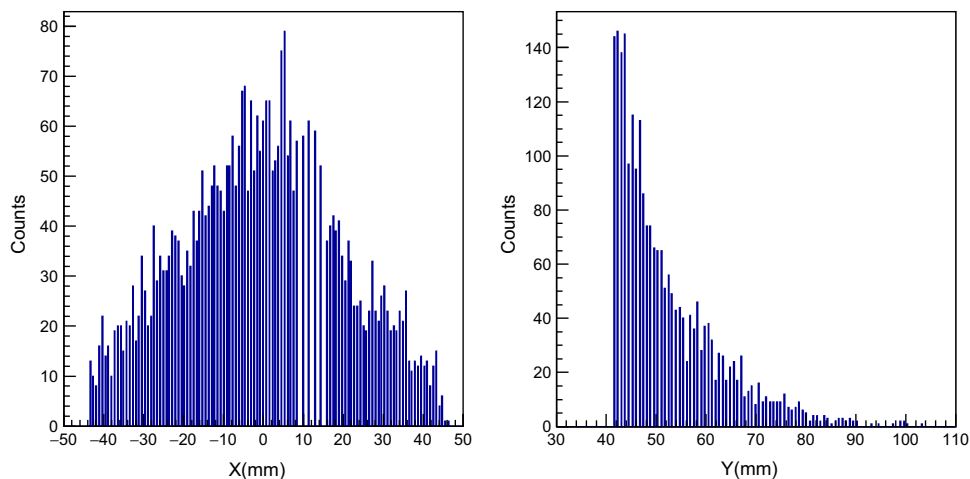


shown in Fig. 5. In this experiment, owing to the limitations of electronics, only three telescopes (Tel1, Tel2, and Tel3) were employed, which satisfied the requirements of this experiment. Figure 6 shows the events of  $X$  and  $Y$  positions in Tel1. Although some channels of a pre-amplifier did not operate during the experiment, the rationality of the performance of the detector system was confirmed.

The  $^{11}\text{Be}$  beam was produced through the fragmentation reactions of  $^{13}\text{C}$  primary beam at 54.2 MeV/nucleon, which was separated by the HIRFL, bombarding on a 4500  $\mu\text{m}$  beryllium target located at T0 of RIBLL. To enhance the purity of  $^{11}\text{Be}$ , an Al wedge with the thickness of 1500  $\mu\text{m}$  was placed at the first focal plane of the RIBLL and used as a degrader. To regulate the energy, three replaceable and thinner Al degraders were installed at the second focal plane of RIBLL. To identify particles from the contaminants, a time-of-flight (TOF) detector was used, in which two plastic scintillation detectors of 50 and 100  $\mu\text{m}$  were installed at T1 and T2 with a flight path of 17 m. Two DSSDs with 16 horizontal and 16 vertical strips were arranged in this experiment to obtain the precise position and direction of the RIBs. These two DSSDs with the thicknesses of 68 and 87  $\mu\text{m}$  in front of the target are shown in Fig. 5, and are denoted Sistrip1 and Sistrip2, respectively. They are set away from the lead target at the distances of 663.4 and 367 mm, respectively. A self-supporting foil lead target with the thickness of 7.85  $\text{mg}/\text{cm}^2$  was used in this experiment.

The detector array was calibrated in three steps. The first stage involved the calibration of the device in the running configuration using a precision pulser with a charge terminator. In the second stage, a series of fragmentation

**Fig. 6** (Color online)  $X$  and  $Y$  positions obtained with DSSD in Tell for this experiment. The strip width is 0.76 mm in both  $X$  and  $Y$  directions

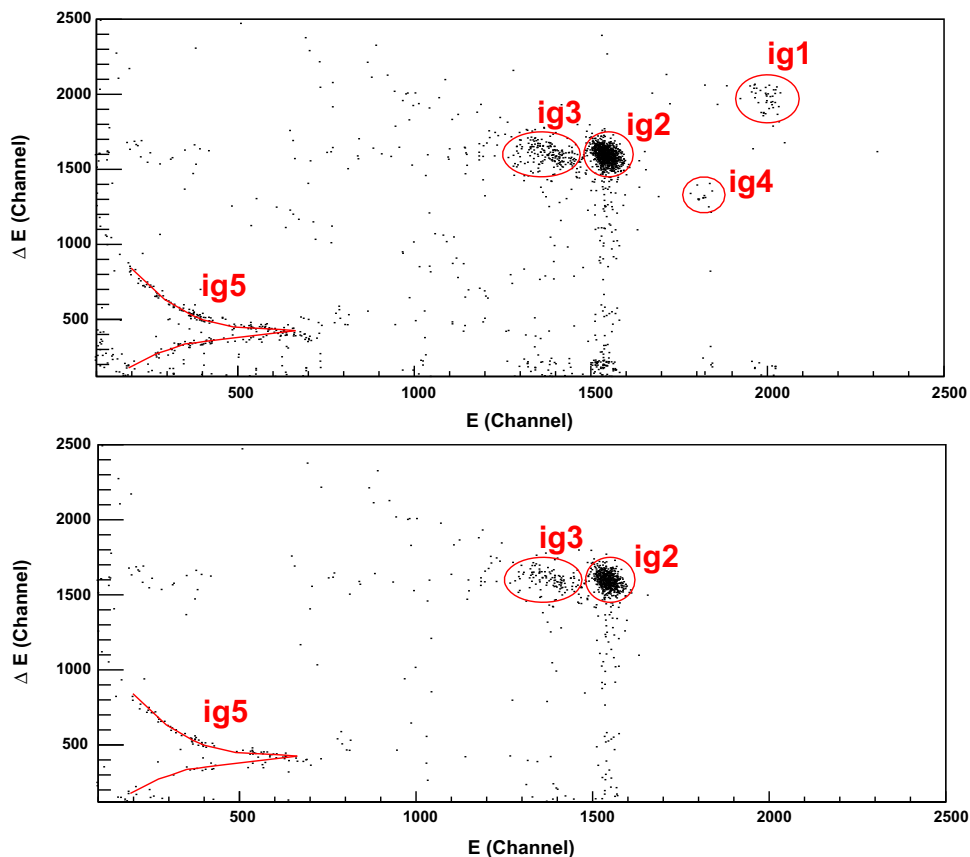


beams was used and each detector was repositioned to allow the beam to be implanted directly into the telescope. The  $^{11}\text{Be}$  Beam with 54.2 MeV/nucleon was separated by RIBLL after the primary beam, provided by the HIRFL, bombarding the Be target at the T0 of RIBLL. Reaction products from projectile fragmentation were subsequently selected according to the magnetic rigidity. The beams can be used to calibrate both  $\Delta E$  detectors and E detectors.

Finally, a  $^{241}\text{Am}$   $\alpha$ -particle source was used to calibrate the DSSDs.

In Fig. 7, the upper panel shows the typical  $\Delta E - E$  particle identification spectrum obtained with a single pixel for the reaction of  $^{11}\text{Be}$  on a  $^{208}\text{Pb}$  target at  $E_{\text{lab}} = 140$  MeV. The spectrum shows the original situation with no selection of the incident beams and ig1, ig2, ig3, and ig5 are recognized as  $^{12}\text{B}$ ,  $^{11}\text{Be}$ ,  $^{10}\text{Be}$ , and  $^4\text{He}$ , respectively. It can be observed that the contaminant ig4, which represents

**Fig. 7** (Color online) Spectrum of  $\Delta E - E$  for a single pixel of a forward telescope for the reaction  $^{11}\text{Be} + ^{208}\text{Pb}$  at 140 MeV. The upper panel shows the original beam, and the lower panel shows the beam subject in the frame of a cut on the TOF



$^{10}\text{Be}$ , originates from the ion beam. Further, the tails represent only very small portions of the incident particles, and they can be cut off by means of the TOF obtained by the upstream beam monitors and the beam spot at the target position, which is a beam profile projected from Sistrup1 and Sistrup2 positions. The resulting beam contents are shown in the lower panel of Fig. 7. The contaminants have been removed except for a very small portion of  $^4\text{He}$ , which has no influence on  $^{11}\text{Be}$  and  $^{10}\text{Be}$  data. A preliminary angular distribution of elastic scattering and breakup without normalization and detection efficiency obtained using Te11 is shown in Fig. 8. It shows that the detector array can measure the events of elastic scattering and breakup simultaneously, which satisfies the design requirements.

## 6 Summary and conclusions

In this paper, the design and construction of a new charged-particle detector system are described and applied for measuring the charged particles induced by  $^{11}\text{Be}$  beam at energies three times above the Coulomb barrier. It is a new compact charged-particle silicon detector array based on two-stage detector telescopes, which consist of a DSSD of thickness 150  $\mu\text{m}$  and an SSD of thickness 1500  $\mu\text{m}$ . With a large solid angle, the detector system can be used for the reactions induced by the low-intensity beam. The three different types of DSSDs used in the new detector system have an angular resolution ranging from  $\Delta\theta = 0.15^\circ$  to  $1^\circ$ , depending on the distance from the reaction

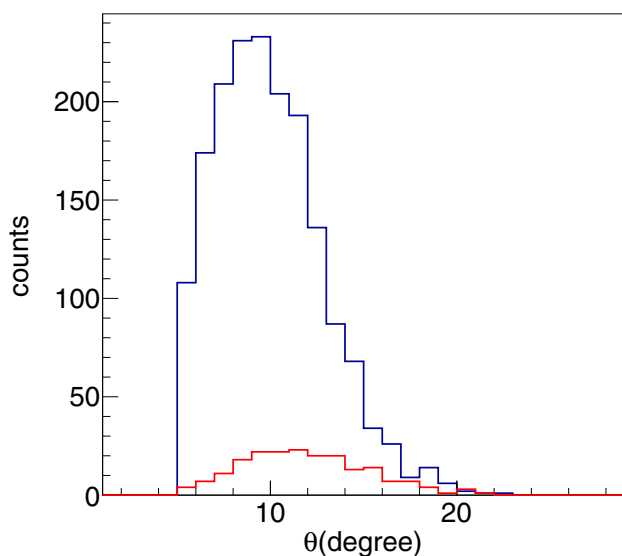


**Fig. 8** (Color online) Angular distribution of elastic scattering of  $^{11}\text{Be}$  obtained using Te11 is shown by the blue line, whereas the corresponding breakup events of  $^{10}\text{Be}$  are shown by the red line

target. The performance of the DSSDs and SSDs of the detector array was initially tested with an  $\alpha$  source. A remarkable energy resolution (FWHM) of each detector of approximately 1% was obtained at  $E = 5.486\text{MeV}$ . Subsequently, the detector system was commissioned on the RIBLL at the HIRFL for the experiment of the elastic scattering of  $^{11}\text{Be} + ^{208}\text{Pb}$  above the Coulomb barrier. The measurement results are consistent with the Monte Carlo simulation.

## References

- I. Tanihata, O. Hashimoto, Y. Shida, Measurements of interaction cross sections and nuclear radii in the light p-shell region. *Phys. Rev. Lett.* **55**, 2676–2679 (1985). <https://doi.org/10.1103/PhysRevLett.55.2676>
- T. Otsuka, T. Suzuki, J. Holt, Three-body forces and the limit of oxygen isotopes. *Phys. Rev. Lett.* **105**, 032501 (2010). <https://doi.org/10.1103/PhysRevLett.105.032501>
- D. Suzuki, H. Iwasaki, D. Beaumel, Breakdown of the  $Z = 8$  shell closure in unbound  $^{12}\text{O}$  and its mirror symmetry. *Phys. Rev. Lett.* **103**, 152503 (2009). <https://doi.org/10.1103/PhysRevLett.103.152503>
- W.H. Ma, J.S. Wang, Y.Y. Yang, Experimental study of the  $^9\text{Li}$  breakup reaction on Pb target. *Nucl. Sci. Tech.* **28**, 177 (2017). <https://doi.org/10.1007/s41365-017-0334-4>
- J.J. Kolata, V. Guimarães, E.F. Aguilera, Elastic scattering, fusion, and breakup of light exotic nuclei. *Eur. Phys. J. A.* **52**, 123 (2016). <https://doi.org/10.1140/epja/i2016-16123-1>
- B. Jonson, Light dripline nuclei. *Phys. Rep.* **389**, 1–59 (2004). <https://doi.org/10.1016/j.physrep.2003.07.004>
- K.A. Li, Y.L. Ye, Recent development in experimental RIB physics. *Nucl. Tech.* **37**(10), 100501 (2014). <https://doi.org/10.11889/j.0253-3219.2014.hjs.37.100501>. (in Chinese)
- S. Wang, Electron scattering facility for short-lived nuclei at RIKEN. *Nucl. Tech.* **37**(10), 100523 (2014). <https://doi.org/10.11889/j.0253-3219.2014.hjs.37.100523>. (in Chinese)
- Y. Blumenfeld, F. Auger, J.E. Sauvestre et al., MUST: a silicon strip detector array for radioactive beam experiments. *Nucl. Instrum. Methods Phys. Res. Sect. A* **421**, 471–491 (1999). [https://doi.org/10.1016/S0168-9002\(98\)01178-4](https://doi.org/10.1016/S0168-9002(98)01178-4)
- E. Pollaco, D. Beaumel, P. Roussel-Chomaz, MUST2: a new generation array for direct reaction studies. *Eur. Phys. J. A* **25**(s01), 287–288 (2005). <https://doi.org/10.1140/epjad/i2005-06-162-5>
- M. Labiche, W.N. Catford, R.C. Lemmon et al., TIARA: a large solid angle silicon array for direct reaction studies with radioactive beams. *Nucl. Instrum. Methods Phys. Res. Sect. A* **614**, 439–448 (2010). <https://doi.org/10.1016/j.nima.2010.01.009>
- G. Marquinez-Durán, L. Acosta, R. Berjillos et al., GLORIA: a compact detector system for studying heavy ion reactions using radioactive beams. *Nucl. Instrum. Methods Phys. Res. Sect. A* **755**, 69–77 (2014). <https://doi.org/10.1016/j.nima.2014.04.002>
- G.L. Zhang, Y.J. Yao, G.X. Zhang, A detector setup for the measurement of angular distribution of heavy-ion elastic scattering with low energy on RIBLL. *Nucl. Sci. Tech.* **28**, 104 (2017). <https://doi.org/10.1007/s41365-017-0249-0>
- L.J. Sun, X.X. Xu, C.J. Lin et al., A detection system for charged-particle decay studies with a continuous-implantation method.

- Nucl. Instrum. Methods Phys. Res. Sect. A **807**, 1–7 (2015). <https://doi.org/10.1016/j.nima.2015.09.039>
15. X.X. Xu, Fanurs C.E. Teh, C.J. Lin et al., Characterization of CIAE developed double-sided silicon strip detector for charged particles. Nucl. Sci. Tech. **29**, 73 (2018). <https://doi.org/10.1007/s41365-018-0406-0>
  16. T. Davinson, W. Bradfield-Smith, S. Cherubini et al., Louvain–Edinburgh Detector Array (LEDA): a silicon detector array for use with radioactive nuclear beams. Nucl. Instrum. Methods Phys. Res. Sect. A **454**, 350–358 (2003). [https://doi.org/10.1016/S0168-9002\(00\)00479-4](https://doi.org/10.1016/S0168-9002(00)00479-4)
  17. A.N. Ostrowski, S. Cherubini, T. Davinson et al., A double sided silicon strip detector for radioactive nuclear beam experiments. Nucl. Instrum. Methods Phys. Res. Sect. A **480**, 448–455 (2002). [https://doi.org/10.1016/S0168-9002\(01\)00954-8](https://doi.org/10.1016/S0168-9002(01)00954-8)
  18. Z.Y. Sun, W.L. Zhan, Z.Y. Guo et al., Separation and identification of isotopes produced from  $^{20}\text{Ne} + \text{Be}$  reaction by radioactive ion beam line in Lanzhou. Chin. Phys. Lett. **15**(11), 790–792 (1998). <https://doi.org/10.1088/0256-307X/15/11/004>
  19. Z.Y. Sun, W.L. Zhan, Z.Y. Guo et al., RIBLL, the radioactive ion beam line in Lanzhou. Nucl. Instrum. Methods Phys. Res. Sect. A **503**, 496 (2003). [https://doi.org/10.1016/S0168-9002\(03\)01005-2](https://doi.org/10.1016/S0168-9002(03)01005-2)
  20. J.W. Xia, W.L. Zhan, B.W. Wei et al., The heavy ion cooler-storage-ring project (HIRFL-CSR) at Lanzhou. Nucl. Instrum. Methods Phys. Res. Sect. A **488**, 11–25 (2002). [https://doi.org/10.1016/S0168-9002\(02\)00475-8](https://doi.org/10.1016/S0168-9002(02)00475-8)
  21. W.L. Zhan, H.S. Xu, G.Q. Xiao et al., Progress in HIRFL-CSR. Nucl. Phys. A **834**, 694c–700c (2010). <https://doi.org/10.1016/j.nuclphysa.2010.01.126>
  22. S. Agostinelli, J. Allison, K. Amako et al., Geant4-a simulation toolkit. Nucl. Instrum. Methods Phys. Res. Sect. A **506**, 250–303 (2003). [https://doi.org/10.1016/S0168-9002\(03\)01368-8](https://doi.org/10.1016/S0168-9002(03)01368-8)
  23. J. Allison, K. Amako, J. Apostolakis, Geant4 developments and applications. IEEE Trans. Nucl. Sci. **53**, 270–278 (2006). <https://doi.org/10.1109/TNS.2006.869826>
  24. <http://geant4.cern.ch>, 2014. <http://geant4.cern.ch>